Journal of
Applied Crystallography
ISSN 0021-8898
Editor: **Anke R. Pyzalla**

Transformations for monoclinic crystal symmetry in texture analysis

Siegfried Matthies and Hans-Rudolf Wenk

J. Appl. Cryst. (2009). **42**, 564–571

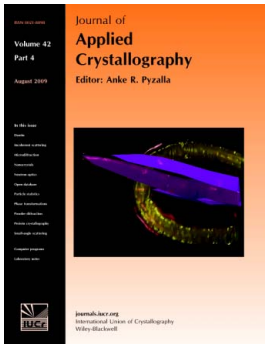

Journal of
Applied Crystallography
ISSN 0021-8898

Received 23 March 2009
Accepted 14 May 2009

Transformations for monoclinic crystal symmetry in texture analysis

Siegfried Matthies[a]‡ and Hans-Rudolf Wenk[b]*

[a]Joint Institute for Nuclear Research, Frank Laboratory of Neutron Physics,141980 Dubna, Moscow Region, Russian Federation, and [b]Department of Earth and Planetary Science, University of California, Berkeley CA 94720, USA. Correspondence e-mail: wenk@berkeley.edu

Monoclinic crystals can be described in two settings: in the first setting the C_2 rotation axis is parallel to the z axis and in the second setting it is parallel to the y axis. Transformations of lattice parameters, Miller and zone indices, and atomic coordinates is straightforward; the situation is far more complex for texture analysis with orientation distributions and corresponding representations. This article gives explicit transformations that need to be applied, not only for texture analysis but also for calculations of physical properties of materials with preferred orientation. In texture research the relationship between the Cartesian crystal coordinate system and the unit cell must be unambiguously defined and a uniform convention is desirable.

1. Introduction

When it comes to crystal symmetry there is a rigorous system that was developed centuries ago, establishing lattice types, point groups and space groups with clearly defined conventions, and yet there are some aspects that can cause considerable pain, not so much for single crystals, but when it comes to crystal aggregates and texture analysis. In this article we analyze the issue of monoclinic settings and corresponding transformations.

For all crystals with a symmetry axis, the (crystallographic) z axis is chosen as the unique axis, except for the monoclinic system, where it is either the z axis (parallel to **c**, first setting) or the y axis (parallel to **b**, second setting). The origin of this confusion lies in mineralogy, where lattice planes are traditionally defined on the basis of morphology and the second setting is used. For example, in mica, the 'basal' plane (001) is an excellent cleavage plane but not the monoclinic mirror plane. In pyroxenes, [001] is the direction of the silicate chains but not the monoclinic rotation axis. Likewise, in monoclinic feldspars, the (010) cleavage must correspond to the equivalent cleavage plane in triclinic feldspars. Many crystallographic data sets for monoclinic crystals (crystallographic information files or CIFs) use the second setting. The early editions of the *International Tables for the Determination of Crystal Structures* (1935) only use the setting with the y axis. Later, physicists introduced the more sensible setting with the z axis, which became known as the first setting, and later editions of the *International Tables for Crystallography* (1965) list both settings. However, even today, most new structures are described in the second setting.

Whatever the reason for the diversity, the need often arises to transform from one to the other system. This is relatively straightforward when it comes to lattice parameters, Miller and zone indices, and atomic positions and has been clearly described in the newer *International Tables for X-ray Crystallography* (1969, Vol. 1). However, what about defining the orientation of a monoclinic crystal relative to the sample coordinates, or the orientation distribution of Euler angles in texture analysis? Furthermore, what about elastic properties of monoclinic crystals described with tensor notation? Most texture research ignores monoclinic crystals. Some systems, such as the analytical software *Beartex* (Wenk *et al.*, 1998) and the Rietveld system *MAUD* (*Materials Analysis Using Diffraction*; Lutterotti *et al.*, 1997), use the first setting. The Los Alamos polycrystal plasticity code (VPSC; Lebensohn & Tome, 1994) also uses the first setting. However, electron backscatter diffraction systems such as *HKL* (Schmidt & Olesen, 1989) use the second setting. For all crystals except monoclinic there is a straightforward interface for data exchange. Here we provide recipes for conversions from the first setting to the second setting, and *vice versa*, and illustrate them with examples.

2. Two coordinate lattice systems

Fig. 1 shows a monoclinic unit cell with lattice vectors **a**, **b**, **c** assigned for the first (Fig. 1*a*) and the second setting (Fig. 1*b*). There are three point groups in this crystal system [C_2 (2), C_s (m), C_{2h} (2/m)]. For all these point groups a diadic C_2 axis exists in the case of normal scattering.

The C_2 rotation axis is parallel to either **c** or **b**. In each case the lattice vectors are assigned so that the vector triplet obeys the condition $\mathbf{a} \cdot (\mathbf{b} \times \mathbf{c}) > 0$ ('right handed lattice vector triplet'). In order to avoid additional ambiguity, two further

‡ Permanent address: Mueller-Berset-Strasse 3, 01309 Dresden, Germany.

(>, <) conditions have to be specified: $a < (>)\ b$ and $\gamma < (>)\ \pi/2$. Fig. 2 illustrates the second variant (II) for the first setting with the choice $\gamma' > \pi/2$, in order to demonstrate that the resulting (**a**, **b**, **c**) triplet cannot be derived from the $\gamma' < \pi/2$ triplet of Fig. 1(*a*) using the C_2 symmetry of the crystal cell. Consequently, there will be different results describing the orientation of the lattice cell for an outside viewer. We will return to these considerations in more detail in §3.

There are various rules for the conventional orientation of the crystal lattice (*e.g.* Donnay, 1943), but as long as the lattice parameters are clearly defined and the unit cell is described in a right-handed lattice vector triplet, the relative values of *a*, *b* and *c*, as well as the use of acute or obtuse angles, do not influence any of the following discussions. For monoclinic settings, $a' \neq b'$ and $0 < \gamma' < 180^\circ$ (and $\neq 90^\circ$), and correspondingly $a'' \neq c''$ and $0 < \boldsymbol{\beta}'' < 180^\circ$ (and $\neq 90^\circ$). With such conventions and definitions the conversion of lattice parameters or lattice-vector-related quantities between the two settings is straightforward:

$$1 \rightarrow 2: \quad \begin{aligned} &a'' = b', \quad b'' = c', \quad c'' = a', \\ &\boldsymbol{\alpha}'' = 90^\circ, \quad \boldsymbol{\beta}'' = \boldsymbol{\gamma}', \quad \boldsymbol{\gamma}'' = 90^\circ, \end{aligned} \tag{1a}$$

$$2 \rightarrow 1: \quad \begin{aligned} &a' = c'', \quad b' = a'', \quad c' = b'', \\ &\boldsymbol{\alpha}' = 90^\circ, \quad \boldsymbol{\beta}' = 90^\circ, \quad \boldsymbol{\gamma}' = \boldsymbol{\beta}''. \end{aligned} \tag{1b}$$

Correspondingly, the Miller indices (*hkl*) transform as

$$1 \rightarrow 2: \quad h'' = k', \quad k'' = l', \quad l'' = h', \tag{2a}$$

$$2 \rightarrow 1: \quad h' = l'', \quad k' = h'', \quad l' = k'', \tag{2b}$$

and the zone indices [*uvw*] as

$$1 \rightarrow 2: \quad u'' = v', \quad v'' = w', \quad w'' = u', \tag{3a}$$

$$2 \rightarrow 1: \quad u' = w'', \quad v' = u'', \quad w' = v'', \tag{3b}$$

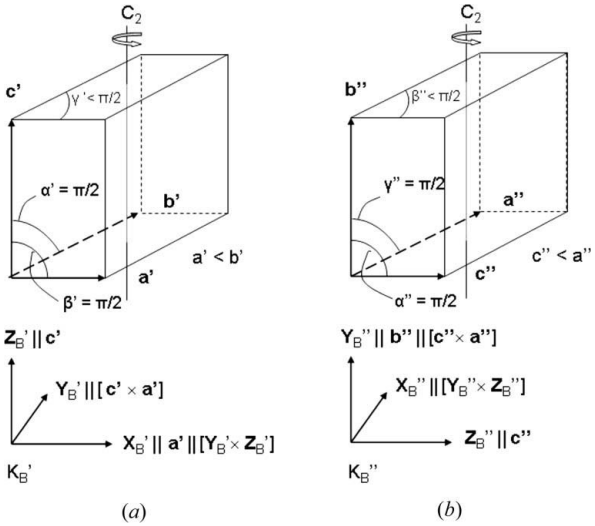

Figure 1
Monoclinic unit cell with (**a**, **b**, **c**) triplets assigned for (*a*) the first setting and (*b*) the second setting and the corresponding crystal coordinate systems K_B following prescription (5).

and a similar transformation applies to atomic coordinates *x*, *y*, *z*:

$$1 \rightarrow 2: \quad x'' = y', \quad y'' = z', \quad z'' = x', \tag{4a}$$

$$2 \rightarrow 1: \quad x' = z'', \quad y' = x'', \quad z' = y''. \tag{4b}$$

Of course, we will obtain the same characteristic *d* spacings of *hkl*-specific crystal planes, introducing into the explicit $d(hkl; a, b, c; \boldsymbol{\alpha}, \boldsymbol{\beta}, \boldsymbol{\gamma})$ relation the set of $(h'\ k'\ l'; a', b', c'; \boldsymbol{\alpha}', \boldsymbol{\beta}', \boldsymbol{\gamma}')$ or $(h''\ k''\ l''; a'', b'', c''; \boldsymbol{\alpha}'', \boldsymbol{\beta}'', \boldsymbol{\gamma}'')$ data, if both are related by equations (1) and (2).

3. Orientation angles

The orientation of a crystal relative to the sample coordinates is generally specified by placing Cartesian coordinate systems in the crystal (K_B) and in the sample (K_A) and expressing the relative orientation of the two with three Euler angles that correspond to rotations to bring the coordinate systems to coincidence. From a first view, the determination of the orientation of a right-handed system K_B [with $\mathbf{X}_B \cdot (\mathbf{Y}_B \times \mathbf{Z}_B) = +1$; $X_B, Y_B, Z_B = 1$], relative to an other right-handed system K_A, seems to be simple, using, for example, the well defined prescription of how K_A can be oriented parallel to K_B by three successive rotations.

Whereas the problem of how to fix K_A (the sample coordinate system) in the sample is our free choice, the determination of a crystal coordinate system K_B in each crystal in the given polycrystalline sample may be a nontrivial problem. Only a well defined K_B specification leads to an unambiguous description of an 'orientation' $g = g(K_B \leftarrow K_A) \equiv g^{B \leftarrow A}$. The K_B prescription is related to the crystal lattice of the substance under consideration.

A unique prescription formulated by Haussühl (1983) and based on much earlier conventions (von Fedorow, 1893; Goldschmidt, 1897; *Standards on Piezoelectric Crystals*, 1949) defines how to fix a right-handed Cartesian coordinate system K_B to a commonly non-orthogonal vector triplet (**a**, **b**, **c**) that obeys the condition $\mathbf{a} \cdot (\mathbf{b} \times \mathbf{c}) > 0$:

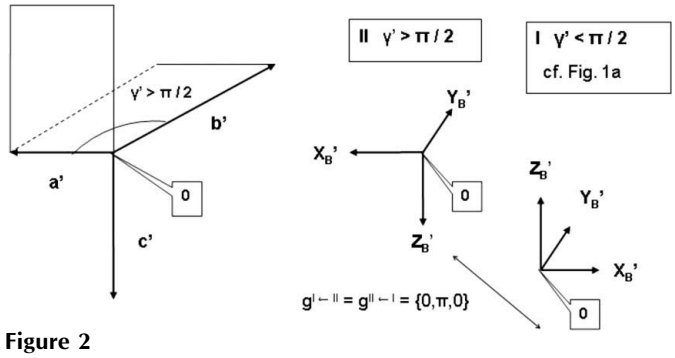

Figure 2
Example of a second variant (II) for the first setting with the choice $\gamma' > \pi/2$, in order to demonstrate that the resulting (**a**, **b**, **c**) triplet cannot be derived from the $(\gamma' > \pi/2)$ triplet of Fig. 1(*a*) using the C_2 symmetry of the crystal cell. Consequently, there will be different results describing the orientation of the lattice cell for an outside viewer. Orientations will be described in more detail in §3.

$$\mathbf{Z}_B \parallel \mathbf{c}, \quad \mathbf{Y}_B \parallel (\mathbf{c} \times \mathbf{a}) \quad \text{and} \quad \mathbf{X}_B = (\mathbf{Y}_B \times \mathbf{Z}_B). \qquad (5)$$

This prescription was not invented for texture analysis but simply follows from the fact that it is mathematically (and computationally) more elegant to describe physical phenomena in a real Euclidian system (Figs. 1 and 2).

There are various conventions for performing these rotations. Bunge (1965) rotates the sample frame into the crystal frame (rotation axes Z_A, $X_{A'}$, $Z_{A''} \parallel Z_B$, angles φ_1, Φ, φ_2). Roe (1965) also rotates the sample frame into the crystal frame, but using a different order of rotations (rotation axes Z_A, $Y_{A'}$, $Z_{A''} \parallel Z_B$, angles Ψ, Θ, Φ), and there are other rotation variants. Here we use Roe angles, but rename them α, β, γ according to the convention adopted by Matthies *et al.* (1987). In the $\{\alpha, \beta, \gamma\}$ variant, which originates from modern theoretical physics (Edmonds, 1957), the angles α and β are directly related to the commonly used spherical angles, describing a direction, *i.e.* β is the polar angle of $\mathbf{Z}_B$ in K_A and α its azimuth. (The Matthies Euler angles α, β, γ are not to be confused with the lattice parameter angles $\boldsymbol{\alpha}$, $\boldsymbol{\beta}$, $\boldsymbol{\gamma}$, always given in bold.) There are simple relationships between the Euler angle conventions that do not depend on crystal symmetry:

$$\alpha = \Psi = \varphi_1 - 90^\circ, \qquad (6a)$$

$$\beta = \Theta = \Phi, \qquad (6b)$$

$$\gamma = \Phi = \varphi_2 + 90^\circ. \qquad (6c)$$

Owing to the ambiguity of how to fix the (**a**, **b**, **c**) triplet [obeying $\mathbf{a} \cdot (\mathbf{b} \times \mathbf{c}) > 0$ and perhaps additional conditions] to the frame of a crystal cell in the non-triclinic case, there are $N_{B\max} > 1$ K_B variants, and correspondingly $N_{B\max}$ different orientations of the considered ('empty') cell relative to a fixed K_A. Using for the prescription information from inside the crystal cell the number N_B of physically equivalent K_B variants describing one cell may be less than $N_{B\max}$.

A unique situation of describing orientations appears by introducing in the orientation space (G space)

$$g \subset G, \quad 0^\circ \le \alpha, \quad \gamma \le 360^\circ, \quad 0 \le \beta \le 180^\circ, \qquad (7)$$

N_B equivalent 'elementary G-space regions', with correspondingly lower $\{\alpha, \beta, \gamma\}$ regions than in equation (7). The problem is how to select the N_B 'true' K_B variants from the $N_{B\max}$ K_B variants ('starting set') [see Table 5.1 of Matthies *et al.* (1987)].

For the monoclinic system of interest, orientation distributions derived from normal scattering data possess a diadic C_2 symmetry with $N_B = N_{B\max} = 2$ [for details see Table 14.1 of Matthies *et al.* (1987)]. Therefore in the monoclinic system (independent of the 'setting' considered) there are two choices for defining physically equivalent K_B and $\underline{K}_B$ systems, as can be seen in Fig. 3.

Comparing the directions of the Z_B and $\underline{Z}_B$ axes in a fixed coordinate system K_A (which determine the corresponding orientation angles α and β), it can be deduced that the two elementary regions for the two settings can be chosen as

$$G_1': \quad 0 \le \alpha \le 360^\circ, \quad 0 \le \beta \le 180^\circ, \quad 0 \le \gamma \le 180^\circ, \quad (7a)$$

$$G_2': \quad 0 \le \alpha \le 360^\circ, \quad 0 \le \beta \le 180^\circ, \quad 180 \le \gamma \le 360^\circ, \quad (7b)$$

$$G_1'': \quad 0 \le \alpha \le 360^\circ, \quad 0 \le \beta \le 90^\circ, \quad 0 \le \gamma \le 360^\circ, \quad (7c)$$

$$G_2'': \quad 0 \le \alpha \le 360^\circ, \quad 90 \le \beta \le 180^\circ, \quad 0 \le \gamma \le 360^\circ. \quad (7d)$$

A spatially fixed vector **r** is described in a given coordinate system K by its x, y, z components, $\mathbf{r} = (x, y, z) \equiv (x_1, x_2, x_3)$. In mathematical operations we consider **r** as a column vector.

Of interest are the relations between the components of one and the same vector described in K_A or K_B for the known orientation $g = g^{B \leftarrow A}$. They can be described by a matrix defined as

$$\mathbf{r}^B = (x_1^B, x_2^B, x_3^B) = g^{B \leftarrow A} \cdot \mathbf{r}^A, \quad x_i^B = \sum_{j=1}^{3} g_{i,j} x_j^A \quad (i = 1, 2, 3), \qquad (8a)$$

$$\mathbf{r}^A = (x_1^A, x_2^A, x_3^A) = g^{A \leftarrow B} \cdot \mathbf{r}^B, \quad x_i^A = \sum_{j=1}^{3} g_{i,j}^{-1} x_j^B. \qquad (8b)$$

Describing the orientation $g^{B \leftarrow A} = \{\alpha, \beta, \gamma\}$ of K_B relative to K_A by the $\{\alpha, \beta, \gamma\}$ variant of Euler angles, together with the corresponding rotation prescription, the angle β denotes the polar angle of $\mathbf{Z}_B$ in K_A and α its azimuth, as already mentioned. γ belongs to the remaining rotation around $\mathbf{Z}_A$ in order to bring the Y axis of the already rotated K_A (with $\mathbf{Z}_A \parallel \mathbf{Z}_B$) into the direction $\mathbf{Y}_B$.

The explicit expression of the g matrix in terms of its matrix elements $g_{i,j}$ is

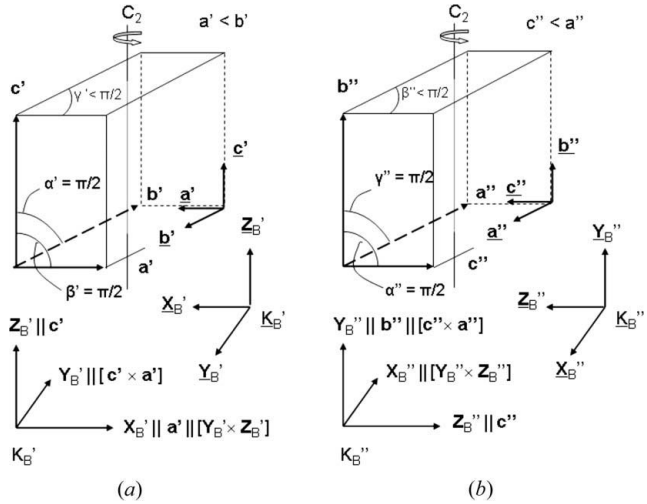

Figure 3
Two ways to place a physically equivalent coordinate system K_B in a monoclinic crystal as a result of the C_2 symmetry. (*a*) First setting K_B' and $\underline{K}_B'$. (*b*) Second setting K_B'' and $\underline{K}_B''$. $\underline{K}_B$ follows from the (**a**, **b**, **c**) triplets shown in the right rear corners. Both triplets (**a**, **b**, **c**) and (**a**, **b**, **c**) obey the definition of the lattice parameters for the monoclinic case and the condition $\mathbf{a} \cdot (\mathbf{b} \times \mathbf{c}) > 0$.

$$g = \begin{pmatrix} \cos\alpha\cos\beta\cos\gamma - \sin\alpha\sin\gamma & \sin\alpha\cos\beta\cos\gamma + \cos\alpha\sin\gamma & -\sin\beta\cos\gamma \\ -\cos\alpha\cos\beta\sin\gamma - \sin\alpha\cos\gamma & -\sin\alpha\cos\beta\sin\gamma + \cos\alpha\cos\gamma & \sin\beta\sin\gamma \\ \cos\alpha\sin\beta & \sin\alpha\sin\beta & \cos\beta \end{pmatrix}. \quad (9)$$

Because g is a (real) unitary matrix, it holds that

$$g_{i,j}^{-1} = g_{j,i} = (g^{B\leftarrow A})_{i,j}^{-1} = g_{i,j}^{A\leftarrow B} = g_{j,i}^{B\leftarrow A}. \quad (10)$$

For $K_A = K_B'$ and $K_B = K_B''$ it follows from Fig. 1 that

$$g(K_B'' \leftarrow K_B') \equiv g^{''\leftarrow'} = \{0, \pi/2, \pi/2\} \quad (11a)$$

and

$$g(K_B' \leftarrow K_B'') \equiv g^{'\leftarrow''} = \{0, \pi/2, \pi/2\}^{-1} = \{\pi/2, \pi/2, \pi\}. \quad (11b)$$

If a transformation of a single orientation $g'' = \{\alpha'', \beta'', \gamma''\}$, given in the second setting, into the first setting $g' = \{\alpha', \beta', \gamma'\}$ is necessary, we use the following relation:

$$\begin{aligned} \{\alpha', \beta', \gamma'\} = g' &= g^{B'\leftarrow A} = g^{B'\leftarrow B''} \cdot g^{B''\leftarrow A} = g^{'\leftarrow''} \cdot g'' \\ &= \{\pi/2, \pi/2, \pi\} \cdot \{\alpha'', \beta'', \gamma''\}. \end{aligned} \quad (12)$$

In order to determine the angles $\{\alpha', \beta', \gamma'\}$ the representation of an orientation g by its matrix [equation (9)] can be used. If the matrix elements of g are known, from $g_{3,3}$ it follows that

$$\begin{aligned} \beta &= \arccos(g_{3,3}), \ 0 \le \beta \le \pi, \\ \text{with } B &= \sin\beta = (1 - \cos^2\beta)^{1/2} \ge 0. \end{aligned} \quad (13)$$

Using $g_{3,1}$ and $g_{3,2}$ we obtain

$$\alpha = \arccos(g_{3,1}/B), \quad (14a)$$

and

$$\text{for } \operatorname{sign}(\sin\alpha) = \operatorname{sign}(g_{3,2}) < 0 \text{ take } (2\pi - \alpha) \text{ for } \alpha. \quad (14b)$$

Correspondingly we obtain γ by

$$\gamma = \arccos(-g_{1,3}/B), \text{ or } (2\pi - \gamma) \text{ for } \operatorname{sign}(g_{2,3}) < 0. \quad (15)$$

For $\beta = 0, \pi$ ($B = 0$) we can use the relations $\{\alpha, 0, \gamma\} = \{\alpha + \gamma, 0, 0\}$, $\{\alpha, \pi, \gamma\} = \{\alpha - \gamma, \pi, 0\}$. After defining $\gamma \equiv 0$, it is sufficient to determine α only. For the case $\gamma = 0$ and $\beta = 0, \pi$, by equation (9) it follows that $g_{2,1} = -\sin\alpha$ and $g_{2,2} = \cos\alpha$, which leads to

$$\begin{aligned} \alpha = \arccos(g_{2,2}), \text{ and for } \operatorname{sign}(\sin\alpha) = \operatorname{sign}(-g_{2,1}) < 0 \\ \text{take } (2\pi - \alpha) \text{ for } \alpha. \end{aligned} \quad (16)$$

Now equation (12) can be rewritten (using $\alpha' \equiv \underline{\alpha}' + \alpha''$) as

$$\begin{aligned} \{\alpha', \beta', \gamma'\} &= \{\pi/2, \pi/2, \pi\}\{0, \beta'', \gamma''\}\{\alpha'', 0, 0\} \\ &= \{\underline{\alpha}', \beta', \gamma'\}\{\alpha'', 0, 0\} = \{\underline{\alpha}' + \alpha'', \beta', \gamma'\}. \end{aligned} \quad (17)$$

The $g^{'\leftarrow''} = \{\pi/2, \pi/2, \pi\}$ matrix has the form $g_{i,j}^{'\leftarrow''} = 0$, except $g_{1,3}^{'\leftarrow''} = g_{2,1}^{'\leftarrow''} = g_{3,2}^{'\leftarrow''} = 1$, and for the matrix of interest $\kappa' \equiv \{\underline{\alpha}', \beta', \gamma'\} = \{\pi/2, \pi/2, \pi\}\{0, \beta'', \gamma''\}$ it follows that

$$\begin{aligned} \kappa_{3,3}' &= \sin\beta''\sin\gamma'', \quad \kappa_{3,1}' = -\cos\beta''\sin\gamma'', \\ \kappa_{3,2}' &= \cos\gamma'', \quad \kappa_{1,3}' = \cos\beta'', \quad \kappa_{2,3}' = -\sin\beta''\cos\gamma'', \\ \kappa_{2,2}' &= \sin\gamma'', \quad \kappa_{2,1}' = \cos\beta''\cos\gamma''. \end{aligned} \quad (18)$$

The explicit relations for obtaining α', β' and γ' from α'', β'' and γ'' are, using $\alpha' = \underline{\alpha}' + \alpha''$,

$$\beta' = \arccos(\sin\beta''\sin\gamma''), \quad B' = [1 - (\cos\beta')^2]^{1/2}, \quad (19a)$$

$$\begin{aligned} \underline{\alpha}' &= \arccos(-\cos\beta''\sin\gamma''/B') \\ &\text{or } (2\pi - \underline{\alpha}') \text{ for } \operatorname{sign}(\cos\gamma'') < 0, \end{aligned} \quad (19b)$$

$$\begin{aligned} \gamma' &= \arccos(-\cos\beta''/B') \\ &\text{or } (2\pi - \gamma') \text{ for sign } (-\sin\beta''\cos\gamma'') < 0. \end{aligned} \quad (19c)$$

For $\beta' = 0, \pi$ ($\beta'' = \pi/2$, and $\gamma'' = \pi/2$ or $3\pi/2$), since $\gamma' \equiv 0$ it follows that

$$\underline{\alpha}' = \arccos(\sin\gamma'') = 0 \text{ or } \pi. \quad (19d)$$

Vice versa, for obtaining orientations in the second setting from values in the first setting we have

$$\begin{aligned} \{\alpha'', \beta'', \gamma''\} = g'' &= g^{B''\leftarrow A} = g^{B''\leftarrow B'} \cdot g^{B'\leftarrow A} = g^{''\leftarrow'} \cdot g' \\ &= \{0, \pi/2, \pi/2\} \cdot \{\alpha', \beta', \gamma'\}, \end{aligned} \quad (20)$$

and correspondingly, using $\alpha'' \equiv \underline{\alpha}'' + \alpha'$

$$\beta'' = \arccos(-\sin\beta'\cos\gamma'), \quad B'' = [1 - (\cos\beta'')^2]^{1/2}, \quad (21a)$$

$$\begin{aligned} \underline{\alpha}'' &= \arccos(\cos\beta'\cos\gamma'/B'') \\ &\text{or } (2\pi - \underline{\alpha}'') \text{ for } \operatorname{sign}(\sin\gamma') < 0, \end{aligned} \quad (21b)$$

$$\begin{aligned} \gamma'' &= \arccos(-\sin\beta'\sin\gamma'/B'') \\ &\text{or } (2\pi - \gamma'') \text{ for } \operatorname{sign}(\cos\beta') < 0. \end{aligned} \quad (21c)$$

For $\beta'' = 0, \pi$, since $\gamma'' \equiv 0$ it follows that

$$\underline{\alpha}'' = 3\pi/2. \quad (21d)$$

Note that the short forms of equations (19) and (21) assume that the β parameters on the right side of the equations (*i.e.* β' or β'') are given in the standard region $0 \le \beta \le 180^\circ$.

If for special applications the $g'(\{\alpha'', \beta'', \gamma''\})$ or $g''(\{\alpha', \beta', \gamma'\})$ relations are needed in matrix form, equation (12) or equations (20) and (9) should be used, owing to the simple form of the matrices $\{\pi/2, \pi/2, \pi\}$ and $\{0, \pi/2, \pi/2\}$, which contain only three elements (= 1) not equal to zero.

Because of the nontrivial metrics of the G space, the orientation distributions for a polycrystalline sample may look remarkably different for the two settings and interpretations need to take this into account. An example will be illustrated in a later section.

4. Elastic properties

In texture analysis physical properties are often of interest, and they are obtained by averaging single-crystal properties over the orientation distribution. For monoclinic crystals, the data of physical properties are almost universally given in the second setting (*e.g.* Nye, 1957).

How do we transform, for example, a fourth-rank tensor from the second to the first setting? For a vector given by its vector components $(x, y, z) = (x_1, x_2, x_3)$ the transfer relations follow directly from equations (8*a*) or (8*b*), with $^{A} = ''$, $^{B} = '$ and $g = g'^{\leftarrow''} = \{\pi/2, \pi/2, \pi\}$:

$$x'_i = \sum_{j=1}^{3} g'^{\leftarrow''}_{i,j} x''_j. \tag{22}$$

In analogy with the transfer relations for (*hkl*) [equation (2)], [*uvw*] [equation (3)] and the atomic coordinates [equation (4)] it follows that

$$x' = x'_1 \leftrightarrow z'' = x''_3, \quad y' = x'_2 \leftrightarrow x'' = x''_1, \quad z' = x'_3 \leftrightarrow y'' = x''_2. \tag{23}$$

In the same way a tensor **T** (of the rank *n*) can be transferred simply by considering it as a set of *n* vectors with the tensor (vector) components $Ti_1, i_2, i_3, \ldots, i_n$:

$$T'i_1, i_2, i_3, \ldots, i_n = \sum_{j1,j2,j3,\ldots,jn=1}^{3} g'^{\leftarrow''}_{i1,j1}\, g'^{\leftarrow''}_{i2,j2}\, g'^{\leftarrow''}_{i3,j3} \cdots g'^{\leftarrow''}_{in,jn} \times T''j_1, j_2, j_3, \ldots, j_n. \tag{24}$$

Because of the simple form ($g'^{\leftarrow''}_{i,j} = 0$, except $g'^{\leftarrow''}_{1,3} = g'^{\leftarrow''}_{2,1} = g'^{\leftarrow''}_{3,2} = 1$) of the matrix $g'^{\leftarrow''} = \{\pi/2, \pi/2, \pi\}$ it directly follows that

$$\begin{array}{cccccc} T'(i_1 = 1,2,3), & (i_2 = 1,2,3), & (i_3 = 1,2,3) \cdots & (i_n = 1,2,3) \\ \updownarrow\updownarrow\updownarrow & \updownarrow\updownarrow\updownarrow & \updownarrow\updownarrow\updownarrow & \updownarrow\updownarrow\updownarrow \\ T''(i_1 = 3,1,2), & (i_2 = 3,1,2), & (i_3 = 3,1,2) \cdots & (i_n = 3,1,2). \end{array} \tag{25}$$

A special case are the tensors describing the linear elastic properties (Hooke's law), the stiffness **C** or compliance **S** tensors. Because one is the inverse of the other we only consider the stiffness tensor. **C** is a tensor of rank 4, *i.e.* its original components have the form Ci_1, i_2, i_3, i_4. However, the elastic tensors of crystals possess special symmetries (Nye, 1957). First, considering i_3 and i_4 as j_1 and j_2, there is a pair symmetry ($i \leftrightarrow j$):

$$Ci_1, i_2; j_1, j_2 = Cj_1, j_2; i_1, i_2. \tag{26}$$

Moreover, inside a pair the indices can be exchanged ['$(1 \leftrightarrow 2)$ symmetry']:

$$Ci_1, i_2; j_1, j_2 = Ci_2, i_1; j_1, j_2 = Ci_1, i_2; j_2, j_1. \tag{27}$$

Because of equation (27), from the $3 \times 3 \times 3 \times 3 = 9 \times 9 = 81$ index variants only $(9 \rightarrow 6)$ $6 \times 6 = 36$ *C* components possess independent values. The symmetry [equation (26)] leads finally to only 21 ($J \geq I$; $I, J = 1$–6) independent values of an effective 6×6 symmetric **C** matrix, with the matrix elements $C_{I,J} = C_{J,I}$ for triclinic symmetry. In Voigt's notation (Voigt, 1928; Nye, 1957), connecting *i* or *j* with *I* and *J* we obtain

$$\begin{array}{lcccccc} i_1, i_2 \text{ (or } j_1, j_2\text{):} & 1,1 & 1,2 & 1,3 & 2,2 & 2,3 & 3,3 \\ & & 2,1 & 3,1 & & 3,2 & \\ \updownarrow & & & & & & \\ I(\text{or } J) & 1 & 6 & 5 & 2 & 4 & 3 \end{array} \tag{28}$$

and for the two settings in the monoclinic case it follows that

$$\begin{aligned} C'_{1,1} = C''_{3,3},\ C'_{1,2} = C''_{1,3},\ C'_{1,3} = C''_{2,3},\ C'^{*}_{1,4} = C''^{*}_{3,6},\ C'^{*}_{1,5} = C''^{*}_{3,4},\ C'_{1,6} = C''_{3,5}, \\ C'_{2,2} = C''_{1,1},\ C'_{2,3} = C''_{1,2},\ C'^{*}_{2,4} = C''^{*}_{1,6},\ C'^{*}_{2,5} = C''^{*}_{1,4},\ C'_{2,6} = C''_{1,5}, \\ C'_{3,3} = C''_{2,2},\ C'^{*}_{3,4} = C''^{*}_{2,6},\ C'^{*}_{3,5} = C''^{*}_{2,4},\ C'_{3,6} = C''_{2,5}, \\ C'_{4,4} = C''_{6,6},\ C'_{4,5} = C''_{4,6},\ C'^{*}_{4,6} = C''^{*}_{5,6}, \\ C'_{5,5} = C''_{4,4},\ C'^{*}_{5,6} = C''^{*}_{4,5}, \\ C'_{6,6} = C''_{5,5}. \end{aligned} \tag{29}$$

For monoclinic symmetry the coefficients marked with an asterisk are equal to zero, resulting in 13 independent coefficients.

5. Examples

5.1. Transformation of Euler angles

Assume that we have an orientation $g'_0 = g^{B' \leftarrow A} = \{\alpha' = 0^\circ, \beta' = 0^\circ, \gamma' = 0^\circ\}$ in the first setting, *i.e.* a single crystal with $K'_B \parallel K_A$, and for the lattice parameters we assume $a' = 10$, $b' = 20$, $c' = 30$ Å, $\boldsymbol{\alpha}' = 90$, $\boldsymbol{\beta}' = 90$, $\boldsymbol{\gamma}' = 70^\circ$ in the first setting. Then the polar angles ζ' and azimuths φ' in K'_B of the normals $\mathbf{n}'(h'k'l') = \mathbf{n}'(\zeta', \varphi')$ of the following $(h'k'l')'$ planes are, respectively, $(100)' \rightarrow (90^\circ, 160^\circ)'$; $(010)' \rightarrow (90^\circ, 90^\circ)'$; $(001)' \rightarrow (0^\circ, 0^\circ)'$; $(101)' \rightarrow (72.60^\circ, 160^\circ)'$.

According to $g'_0 = \{0, 0, 0\}$, poles will be seen in the corresponding $(h'k'l')'$ pole figures of the first setting at the above (ζ', φ') positions since $\mathbf{y} = (\zeta^A, \varphi^A) = \mathbf{y}^A = \mathbf{n}^A(h'k'l')' = \mathrm{g}^{A \leftarrow B'} \cdot \mathbf{n}'(h'k'l') = (g^{B' \leftarrow A})^{-1} \cdot \mathbf{n}'(h'k'l') = (g'_0)^{-1} \cdot \mathbf{n}'(h'k'l') = \{0, 0, 0\}^{-1} \cdot \mathbf{n}'(h'k'l') = \{0, 0, 0\} \cdot \mathbf{n}'(\zeta', \varphi') = \mathbf{n}'(\zeta', \varphi') = (\zeta', \varphi')$.

In the second setting the same orientation is described by $g''_0 = g^{B'' \leftarrow A} = g''^{\leftarrow'} g^{B' \leftarrow A} = g''^{\leftarrow'} g'_0 = \{0, \pi/2, \pi/2\}\{0, 0, 0\} = \{0^\circ, 90^\circ, 90^\circ\}$. Using the lattice parameters in the second setting [*cf.* equation (1*a*)] $a'' = 20$, $b'' = 30$, $c'' = 10$ Å, $\boldsymbol{\alpha}'' = 90$, $\boldsymbol{\beta}'' = 70$, $\boldsymbol{\gamma}'' = 90^\circ$, and $(h''k''l'')''$, following from equation (2*a*), we will obtain the corresponding spherical angles of the normal directions $\mathbf{n}''(h''k''l'') = \mathbf{n}''(\zeta'', \varphi'')$ in K''_B: $(001)'' \rightarrow (20^\circ, 180^\circ)''$; $(100)'' \rightarrow (90^\circ, 0^\circ)''$; $(010)'' \rightarrow (90^\circ, 90^\circ)''$; $(011)'' \rightarrow (26.27^\circ, 137.52^\circ)''$.

Transforming these directions into K_A ($\parallel K'_B$ for the given orientation), using the relation $\mathbf{y} = (\zeta^A, \varphi^A) = \mathbf{y}^A = \mathbf{n}^A(h''k''l'') = g^{A \leftarrow B''} \cdot \mathbf{n}''(h''k''l'') = (g^{B'' \leftarrow A})^{-1} \cdot \mathbf{n}''(h''k''l'') = \{0^\circ, 90^\circ, 90^\circ\}^{-1} \cdot \mathbf{n}''(h''k''l'') = \{90^\circ, 90^\circ, 180^\circ\} \cdot \mathbf{n}''(h''k''l'') = \{90^\circ, 90^\circ, 180^\circ\} \cdot \mathbf{n}''(\zeta'', \varphi'')$, the same values ($\zeta^A = \zeta'$, $\varphi^A = \varphi'$) will appear for the spherical angles (ζ^A, φ^A) as if working with the first setting and naming the pole figures $(h'k'l')$ according to the relation (2*a*), $(h'k'l') \leftrightarrow (h''k''l'')$.

Therefore the pole figures themselves (describing in the sample coordinate system K_A the directions and the frequency of the normals of a specific set of lattice planes in the given sample) do not change for different descriptions (name) of the crystal planes that follow from the choice of a certain variant (setting) of the (**a**, **b**, **c**) triplet.

Fig. 4 shows the $(100)'$, $(010)'$ $(001)'$ and $(101)'$ pole figures of the considered monocrystal with the orientation $g'_0 = \{0^\circ, 0^\circ, 0^\circ\}'$ in the first setting, corresponding to the $(001)''$, $(100)''$, $(010)''$ and $(011)''$ pole figures for the orientation $g''_0 = \{0^\circ, 90^\circ, 90^\circ)''$ in the second setting. Because in the first setting the Z'_B axis (directed along the C_2 rotation axis, *cf.* Fig. 1) of the

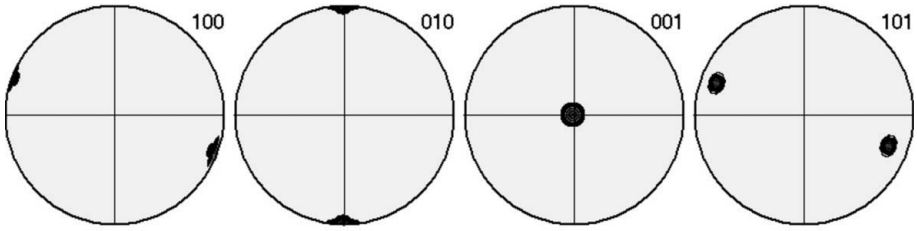

Figure 4
Pole figures $(h'k'l')'$ of a monoclinic single crystal, with the orientation $g^{B'\leftarrow A} = g'_0 = \{0°, 0°, 0°\}'$ in the first setting. The same figures arise for $(h''k''l'')''$ following from equation (2*a*), *i.e.* $(001)''$, $(100)''$, $(010)''$ and $(011)''$, respectively, and describe the orientation of the single crystal in the second setting: $g^{B''\leftarrow A} = g''_0 = \{0°, 90°, 90°\}''$. Equal area projection.

monocrystal is parallel to the Z_A axis of the sample, a C_2 sample symmetry results in this case in two maxima in some pole figures [*e.g.* $(101)'$].

To demonstrate the monoclinic transformations in the orientation space we use two spherical Gaussian texture components (*cf.* Matthies *et al.*, 1987) at $g_0^{I'} = \{40°, 50°, 75°\}'$ and $g_0^{II'} = \{10°, 70°, 25°\}'$ with half-widths (FWHM) $b = 20°$ and intensities 0.125. The lattice parameters are $a' = 3$, $b' = 5$, $c' = 10$ Å, $\boldsymbol{\alpha}' = 90$, $\boldsymbol{\beta}' = 90$, $\boldsymbol{\gamma}' = 65°$.

The plot of the orientation distribution function in the first setting $f'(g')$ is shown in Fig. 5(*a*) by γ' sections ($\gamma' = 15, 25, 35, 65, 75, 85°$). From $f'(g')$, the transformation to $f''(g'')$ follows using $f''(g'') \equiv f'(g') = f'(g'^{\leftarrow\ ''}g'')$ and equation (19). Fig. 5(*b*) shows regions around the γ'' sections that contain the two model components ($\gamma'' = 30, 40, 50°$). As it turns out, the two components in two first setting γ' sections (25 and 75°) are 'far apart' from each other, but both, I and II, lie in the second setting in the same $\gamma'' = 40°$ section. Explicitly it follows from equation (21) that $g_0^{I''} = \{120°, 101°, 139°\}''$. Because of the C_2

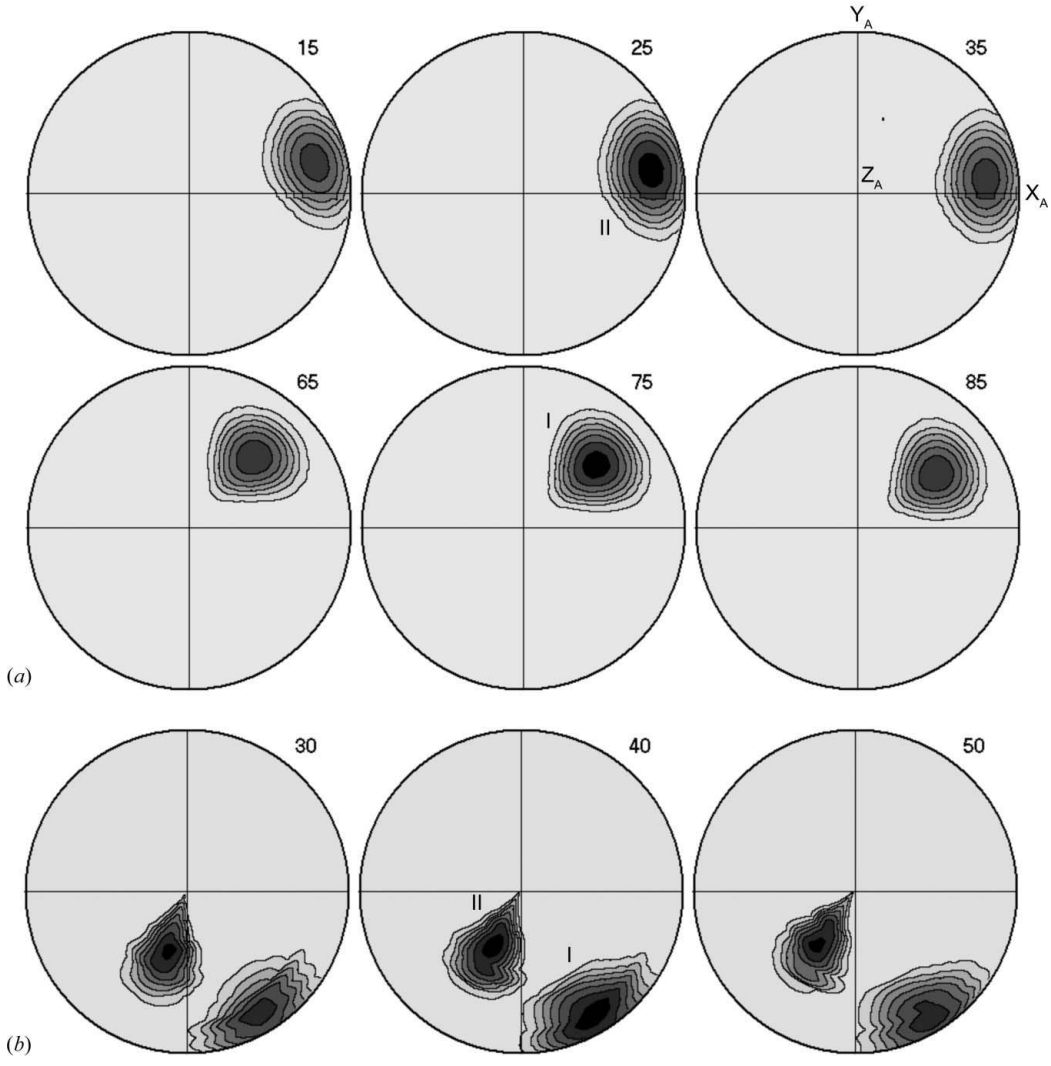

Figure 5
Orientation distribution function of a texture of monoclinic crystals with two texture components, represented in γ sections. $g_0^{I'} = \{40°, 50°, 75°\}'$ and $g_0^{II'} = \{10°, 70°, 25°\}'$, $g_0^{I''} = \{120°, 101°, 139°\}'' \rightarrow \{300°, 79°, 41°\}''$ and $g_0^{II''} = \{64°, 148°, 139°\}'' \rightarrow \{244°, 32°, 41°\}''$. (*a*) First setting: $\gamma' = 15, 25, 35, 65, 75, 85°$. (*b*) Second setting: $\gamma'' = 30, 40, 50°$. Equal area projection, logarithmic pole density scale.

symmetry axis parallel to Y''_B an equivalent component exists at $\{\pi + \alpha'', \pi - \beta'', \pi - \gamma''\}'' \rightarrow \{300^\circ, 79^\circ, 41^\circ\}''$ – the component seen in the figure. The same orientation follows directly from the C_2 equivalent of $g_0^{I\prime}(\{40^\circ, 50^\circ, 75 + 180^\circ\}')$ in the first setting and applying equation (21). Analogously we obtain $g_0^{II''} = \{64^\circ, 148^\circ, 139^\circ\}'' \rightarrow \{244^\circ, 32^\circ, 41^\circ\}''$.

In order to avoid misunderstandings it has to be added that this 'strange behavior' of the positions of the components follows from the limited possibilities to represent the orientation space with its complicated metrics by plane sections (*e.g.* γ sections). In analogy to the pole figures in Fig. 4, which are independent of the setting (K_B variant) used to describe a given orientation, in G space the 'orientation distance' $\omega(g_1, g_2)$ between two orientations g_1 and g_2 also does not depend on the setting chosen to describe g_1 and g_2. Explicitly ω is given by (*cf.* Matthies *et al.*, 1987)

$$\cos\omega = 2(\cos\omega/2)^2 - 1, \tag{30}$$

$$\begin{aligned}\cos\omega/2 = {} & \cos[(\beta_1 - \beta_2)/2]\cos[(\alpha_1 - \alpha_2)/2]\cos[(\gamma_1 - \gamma_2)/2] \\ & - \cos[(\beta_1 + \beta_2)/2]\sin[(\alpha_1 - \alpha_2)/2]\sin[(\gamma_1 - \gamma_2)/2].\end{aligned} \tag{31}$$

For $g_1 = g_0^{I\prime} = \{40^\circ, 50^\circ, 75^\circ\}'$ and $g_2 = g_0^{II\prime} = \{10^\circ, 70^\circ, 25^\circ\}'$ the orientation distance is $\omega = 72^\circ$. The same distance results for $g_1 = g_0^{I''} = \{120^\circ, 101^\circ, 139^\circ\}''$ and $g_2 = g_0^{II''} = \{64^\circ, 148^\circ, 139^\circ\}'$, or for their equivalents $\{300^\circ, 79^\circ, 41^\circ\}''$ and $\{244^\circ, 32^\circ, 41^\circ\}''$.

5.2. Exporting the orientation distribution from the second setting and processing in the first setting

Orientation distributions and corresponding pole figures may be available in the second setting. This is the case for a schist composed of monoclinic muscovite, triclinic chlorite, trigonal quartz, triclinic albite and hexagonal graphite. Only muscovite will be considered here. Muscovite is monoclinic in space group $C2/c$ and the structure is described in a unit cell of the second setting ($a'' = 5.18$, $b'' = 8.96$, $c'' = 20.1$ Å, $\boldsymbol{\alpha}'' = 90$, $\boldsymbol{\beta}'' = 95.66$, $\boldsymbol{\gamma}'' = 90^\circ$.

First the pole figures in the second setting were plotted with the *Beartex* (Wenk *et al.*, 1998) routine *PING* (Fig. 6*a*). Then lattice parameters and Miller indices were converted to the first setting using a new *Beartex* routine *MO21*. With eight pole figures the *WIMV* algorithm was used to obtain an orientation distribution $f'(g')$ (OD). *Beartex* uses the first setting. From the OD several pole figures were calculated with *POLF* and were compared with those from *MAUD* (Fig. 6*b*). As can be clearly seen the agreement is excellent. Note that in the first setting $(h'k'l')'$ (Fig. 6*b*) the pole figure of the cleavage planes of muscovite is $(100)'$.

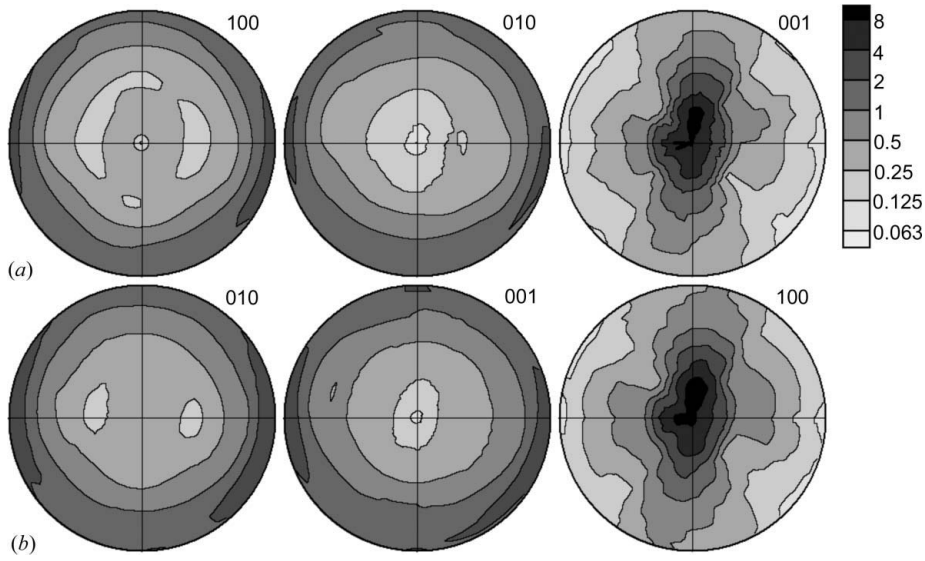

Figure 6
Pole figures for monoclinic muscovite from schist. (*a*) Second setting $(h''k''l'')''$. (*b*) First setting $(h'k'l')'$. The exported pole figures have been converted to the first setting, then processed with *WIMV* in *Beartex* to obtain the OD, and then recalculated. Log scale, equal area projection.

5.3. Elastic properties

The next step was to calculate aggregate elastic properties for muscovite by averaging, applying the 'first setting' OD and supposing that the vector triplet (**a**, **b**, **c**) used for the stiffness data was the same as the above given triplet. For the averaging the published elastic properties for muscovite in the second setting (Vaughan & Guggenheim, 1986) had to be converted using equation (29) (Table 1). Fig. 7(*a*) shows contours of the longitudinal acoustic velocity surface V_P (in km s^{-1}) for the single crystal. It displays the C_2 rotation axis parallel to **c** and $\mathbf{Z}'_B$. The Cartesian crystal coordinate system K_B is indicated. Then the single-crystal tensor was averaged over the orientation distribution using the geometric mean (Matthies *et al.*, 2001) (*Beartex* routine *TENS*; Table 1). Note that the poly-

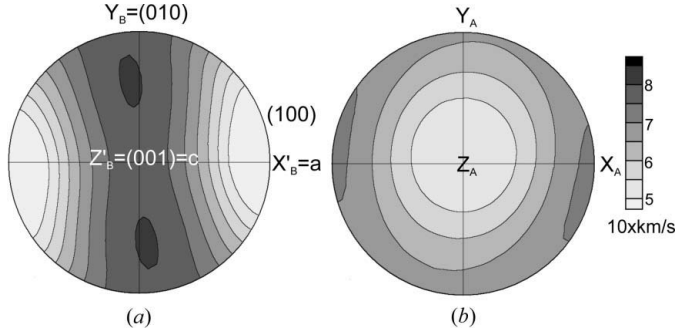

Figure 7
V_P velocity surface for (*a*) muscovite single crystal and (*b*) muscovite in schist. The crystal coordinate system K_B and sample coordinate system K_A are indicated. Equal area projection.

Table 1
Stiffness coefficients (GPa) for muscovite in the second setting (Vaughan & Guggenheim, 1986) and the first setting using the transformation given in equation (29) and for the polycrystal average in schist.

Muscovite single crystal, second setting.

181.0	48.8	25.6	0.0	−14.2	0.0
48.8	178.4	21.2	0.0	1.1	0.0
25.6	21.2	58.6	0.0	1.0	0.0
0.0	0.0	0.0	16.5	0.0	−5.2
−14.2	1.1	1.0	0.0	19.5	0.0
0.0	0.0	0.0	−5.2	0.0	72.0

Muscovite single crystal, first setting.

58.6	25.6	21.2	0.0	0.0	1.0
25.6	181.0	48.8	0.0	0.0	−14.2
21.2	48.8	178.4	0.0	0.0	1.1
0.0	0.0	0.0	72.0	−5.2	0.0
0.0	0.0	0.0	−5.2	16.5	0.0
1.0	−14.2	1.1	0.0	0.0	19.5

Polycrystal average for muscovite in schist.

146.8	39.3	32.5	−0.7	−0.5	−2.4
39.3	125.8	34.8	−3.9	0.2	−1.6
32.5	34.8	73.7	−1.2	−0.2	0.5
−0.7	−0.4	−1.2	26.6	4.8	6.8
−0.5	0.2	−0.2	4.8	26.7	−2.0
−2.4	−1.6	0.5	6.8	−2.0	46.8

crystal tensor is given in the sample coordinate system K_A and is independent of the monoclinic setting. Finally the polycrystal velocity surface was calculated in *VELO* and is plotted in Fig. 7(*b*).

6. Conclusions

The discussion and the examples demonstrate that great care must be applied for texture analysis of monoclinic crystals and nontrivial transformations must be performed. Texture analyses of monoclinic crystals are rare but in some earlier work these complexities have not been properly taken into account (*e.g.* Wenk *et al.*, 2008). Fortunately errors were not very large because the monoclinic lattice angle was close to 90°. This paper presents explicit procedures that need to be followed for texture analysis of monoclinic crystals. Conversions between the two settings have been implemented in both *Beartex* (Wenk *et al.*, 1998) and *MAUD* (Lutterotti *et al.*, 1997). In *MAUD*, structural data are generally imported in the second setting (*e.g.* space group *C*2/*c*:*b*1). Choosing for the space group the first setting (*C*2/*m*:*c*1) automatically converts lattice parameters and atomic coordinates. The conclusions about monoclinic crystal symmetry in this study highlight again the critical importance of a clear and uniform definition of crystal coordinate systems and crystallographic unit cell in texture research such as $\mathbf{Z}_B \parallel \mathbf{c}$, $\mathbf{Y}_B \parallel [\mathbf{c} \times \mathbf{a}]$ and $\mathbf{X}_B = [\mathbf{Y}_B \times \mathbf{Z}_B]$, particularly in triclinic, monoclinic and trigonal systems.

We appreciate the support of this research through grants from the NSF (grant No. EAR 0836402) and DOE (grant No. DE-FG02-05ER15637) as well as CDAC, and also acknowledge discussions on this subject with Daniel Chateigner, Luca Lutterotti and Carlos Tomé.

References

Bunge, H.-J. (1965). *Z. Metallkd.* **56**, 872–974.
Donnay, J. D. H. (1943). *Am. Mineral.* **28**, 313–328.
Edmonds, A. R. (1957). *Angular Momentum in Quantum Mechanics*. Princeton University Press.
Fedorow, E. von (1893). *Z. Krystallogr. Mineral.* **21**, 574–714.
Goldschmidt, V. (1897). *Krystallographische Winkeltabellen*. Berlin: Springer.
Haussühl, S. (1983). *Kristallphysik*. Weinheim: Physik-Verlag.
Lebensohn, R. A. & Tome, C. T. (1994). *Mater. Sci. Eng. A*, **175**, 71–82.
Lutterotti, L., Matthies, S., Wenk, H.-R., Schultz, A. S. & Richardson, J. W. (1997). *J. Appl. Phys.* **81**, 594–600.
Matthies, S., Priesmeyer, H. G. & Daymond, M. R. (2001). *J. Appl. Cryst.* **34**, 585–601.
Matthies, S., Vinel, G. W. & Helming, K. (1987). *Standard Distributions in Texture Analysis*, Vol. I. Berlin: Akademie-Verlag.
Nye, J. F. (1957). *Physical Properties of Crystals*. Oxford: Clarendon Press.
Roe, R.-J. (1965). *J. Appl. Phys.* **36**, 2024–2031.
Schmidt, N. H. & Olesen, N. O. (1989). *Can. Mineral.* **27**, 15–22.
Standards on Piezoelectric Crystals (1949). *Proc. Inst. Radio Eng.* **49**, 1378–1395.
Vaughan, M. T. & Guggenheim, S. (1986). *J. Geophys. Res.* **91**, 4657–4664.
Voigt, W. (1928). *Lehrbuch der Kristallphysik.* Leipzig: Teubner.
Wenk, H.-R., Matthies, S., Donovan, J. & Chateigner, D. (1998). *J. Appl. Cryst.* **31**, 262–269.
Wenk, H.-R., Voltolini, M., Kern, H., Popp, H. & Mazurek, M. (2008). *Leading Edge*, **27**, 742–748.